*Inorg. Chem.* **2008**, *47*, 2837−2848

# Zinc, Cadmium, and Mercury 1,2-Benzenedithiolates with Intramolecular NH···S Hydrogen Bonds

**Koji Baba,[†] Taka-aki Okamura,*[,‡] Hitoshi Yamamoto,[‡] Tetsuo Yamamoto,[‡] and Norikazu Ueyama[‡]**

*Chemical Analysis Research Center, National Institute for Agro-Environmental Sciences, Tsukuba, Ibaraki 305-8604, Japan, and Department of Macromolecular Science, Graduate School of Science, Osaka University, Toyonaka, Osaka 560-0043, Japan*

Received October 14, 2007

Mononuclear Zn, Cd, and Hg 1,2-benzenedithiolates with intramolecular NH···S hydrogen bonds, $[M^{II}\{1,2\text{-}S_2\text{-}3,6\text{-}(RCONH)_2C_6H_2\}_2]^{2-}$ (R = $CH_3$, *t*-Bu; M = Zn, Cd, Hg), were synthesized and characterized by X-ray analysis and spectral measurements. The presence of intramolecular NH···S hydrogen bonds was established by the IR spectra. $^{199}$Hg and $^{113}$Cd nuclear magnetic resonance showed a stabilized four-thiolate coordinated structure and suggested the influence of the NH···S hydrogen bonds to p$\pi$(Hg)−p$\pi$(S) interactions. The NH stretching bands show that the NH···S hydrogen bonds in Cd and Hg complexes are stronger than those in the corresponding Zn complex. These results are supported by theoretical calculations. The experimental and theoretical results suggested that the NH···S hydrogen bond influences the efficient capture of toxic Cd and Hg ions by metallothioneins.

## Introduction

Group 12 metals (Zn, Cd, and Hg) are known to form complexes with various thiolate ligands; in particular, Cd and Hg ions prefer soft thiolate ligands to hard Lewis base donor ligands. Although Cd and Hg are known to inhibit biological functions by strongly binding to cysteine thiolate, protection systems against such heavy metals are also provided. Metallothionein is a cysteine-based protein with a relatively low molecular weight. Toxic metals, such as Cd and Hg, are detoxified by forming numerous metal−sulfur bonds with cysteine thiolates from polypeptide chains.[1,2] In addition to this well-known function, metallothionein is supposed to regulate the transport and storage of essential metal ions, such as Zn and Cu,[3,4] scavenge various radicals and active oxygen species,[5] and be associated with cell proliferation.[6] The molecular structures of metallothioneins were determined by nuclear magnetic resonance (NMR) spectroscopy[7−18] and X-ray analysis.[19,20] In metallothioneins, metals such as Zn and Cd are chelated by four cysteine

* To whom correspondence should be addressed. E-mail: tokamura@chem.sci.osaka-u.ac.jp.
† National Institute for Agro-Environmental Sciences.
‡ Osaka University.

(1) Hamer, D. H. *Annu. Rev. Biochem.* **1986**, *55*, 913–951.
(2) Kagi, J. H. R.; Schaffer, A. *Biochemistry* **1988**, *27*, 8509–8515.
(3) Coleman, J. E. *Annu. Rev. Biochem.* **1992**, *61*, 897–946.
(4) Cavet, J. S.; Borrelly, G. P. M.; Robinson, N. J. *FEMS Microbiol. Rev.* **2003**, *27*, 165–181.
(5) Thornalley, P. J.; Vasak, M. *Biochim. Biophys. Acta* **1985**, *827*, 36–44.
(6) Miles, A. T.; Hawksworth, G. M.; Beattie, J. H.; Rodilla, V. *Crit. Rev. Biochem. Mol. Biol.* **2000**, *35*, 35–70.
(7) Peterson, C. W.; Narula, S. S.; Armitage, I. M. *FEBS Lett.* **1996**, *379*, 85–93.
(8) Narula, S. S.; Brouwer, M.; Hua, Y. X.; Armitage, I. M. *Biochemistry* **1995**, *34*, 620–631.
(9) Capasso, C.; Carginale, V.; Crescenzi, O.; Di Maro, D.; Parisi, E.; Spadaccini, R.; Temussi, P. A. *Structure* **2003**, *11*, 435–443.
(10) Riek, R.; Precheur, B.; Wang, Y. Y.; Mackay, E. A.; Wider, G.; Guntert, P.; Liu, A. Z.; Kagi, J. H. R.; Wuthrich, K. *J. Mol. Biol.* **1999**, *291*, 417–428.
(11) Messerle, B. A.; Schaffer, A.; Vasak, M.; Kagi, J. H. R.; Wuthrich, K. *J. Mol. Biol.* **1990**, *214*, 765–779.
(12) Turner, R. B.; Smith, D. L.; Zawrotny, M. E.; Summers, M. F.; Posewitz, M. C.; Winge, D. R. *Nat. Struct. Biol.* **1998**, *5*, 551–555.
(13) Schultze, P.; Worgotter, E.; Braun, W.; Wagner, G.; Vasak, M.; Kagi, J. H. R.; Wuthrich, K. *J. Mol. Biol.* **1988**, *203*, 251–268.
(14) Blindauer, C. A.; Harrison, M. D.; Robinson, A. K.; Parkinson, J. A.; Bowness, P. W.; Sadler, P. J.; Robinson, N. J. *Mol. Microbiol.* **2002**, *45*, 1421–1432.
(15) Arseniev, A.; Schultze, P.; Worgotter, E.; Braun, W.; Wagner, G.; Vasak, M.; Kagi, J. H. R.; Wuthrich, K. *J. Mol. Biol.* **1988**, *201*, 637–657.
(16) Wang, H.; Zhang, Q.; Cai, B.; Li, H. Y.; Sze, K. H.; Huang, Z. X.; Wu, H. M.; Sun, H. Z. *FEBS Lett.* **2006**, *580*, 795–800.
(17) Zangger, K.; Oz, G.; Otvos, J. D.; Armitage, I. M. *Protein Sci.* **1999**, *8*, 2630–2638.
(18) Munoz, A.; Forsterling, F. H.; Shaw, C. F.; Petering, D. H. *J. Biol. Inorg. Chem.* **2002**, *7*, 713–724.
(19) Robbins, A. H.; McRee, D. E.; Williamson, M.; Collett, S. A.; Xuong, N. H.; Furey, W. F.; Wang, B. C.; Stout, C. D. *J. Mol. Biol.* **1991**, *221*, 1269–1293.
(20) Calderone, V.; Dolderer, B.; Hartmann, H. J.; Echner, H.; Luchinat, C.; Del Bianco, C.; Mangani, S.; Weser, U. *Proc. Natl. Acad. Sci. U.S.A.* **2005**, *102*, 51–56.

10.1021/ic702037k CCC: $40.75 
Published on Web 03/11/2008

thiolates with a tetrahedral coordination geometry[19] and Cu is chelated by two or three thiolates with a linear or trigonal geometry.[20] Titration and spectroscopic experiments suggested tetrahedrally coordinated Hg at low Hg/metallothionein ratios,[21–25] although the metallotioneins containing Hg have not been structurally characterized.

The X-ray crystal structure analysis of rat metallothionein-2 suggested that the coordinating sulfur atoms formed NH···S hydrogen bonds with the amide protons in the polypeptide backbone and with the ammonium protons in the lysine residues.[19] Three NH···S hydrogen bonds interactions in $Cd_3\beta_N$ domains from *Homarus americanus* metallothionein were determined from heteronuclear multiple-quantum coherence (HMQC) experiments.[18] The role of hydrogen bonds in metallothioneins has been discussed using model complexes[26,27] or a modified metallothionein.[28] Walters et al. reported that the NH···S hydrogen bond stabilized the metal-bridging ligand framework.[27] We have systematically synthesized and characterized a series of thiolate complexes with intramolecular NH···S hydrogen bonds.[29–32] $(NEt_4)_2[Co^{II}(S\text{-}2\text{-}t\text{-}BuCONHC_6H_4)_4]$[31] and $(NEt_4)_2[Cu^{I}(S\text{-}2\text{-}t\text{-}BuCONHC_6H_4)_3]$[29] showed strong intramolecular NH···S hydrogen bonds, in which the M−S bond lengths were shorter than those of the corresponding benzenethiolate complexes $(NEt_4)_2[Co^{II}(SC_6H_5)_4]$[33] and $(NEt_4)_2[Cu^{I}(SC_6H_5)_3]$.[34] In the case of Hg ions, weak intramolecular NH···S hydrogen bonds were observed in $Hg^{II}(S\text{-}2\text{-}t\text{-}BuCONHC_6H_4)_2$ with a two-coordinated linear geometry.[30] The intramolecular NH···S hydrogen bond in $[Hg^{II}\{S\text{-}2\text{-}C_{23}H_{36}(OH)_3CONHC_6H_4\}_2]$ lowered the p$K_a$ value of the thiol and prevented the dissociation of the Hg−S bond by water.[32] Recently, we have reported a Hg complex having four thiolate ligands with NH···S hydrogen bonds, $[Hg^{II}(S\text{-}2\text{-}CH_3NHCOC_6H_4)_4]^{2-}$.[35] This complex shows strong NH···S hydrogen bonds that should stabilize the excess negative charge acquired because of the increase in the coordination number. However, this complex shows ligand dissociation equilibrium in solution; thus, the contribution of hydrogen bonds to M−S bonds is not exactly evaluated. Chelation should suppress the dissociation of the ligand. Recently, we have reported a dithiolate ligand with intramolecular NH···S hydrogen bonds to clarify the role of the NH···S hydrogen bonds in molybdenum and tungsten enzymes.[36,37] In this paper, group 12 metal complexes with the dithiolate ligand, $[M^{II}\{1,2\text{-}S_2\text{-}3,6\text{-}(RCONH)_2C_6H_2\}_2]^{2-}$ (R = $CH_3$, *t*-Bu; M = Zn, Cd, Hg), were synthesized and characterized to systematically investigate the effect of the NH···S hydrogen bonds in Zn, Cd, and Hg complexes. Nonsubstituted complexes, $[M^{II}(1,2\text{-benzenedithiolate})_2]^{2-}$ (M = Zn, Cd, Hg), were also synthesized as standard compounds.

## Experimental Section

**Materials.** All reactions were carried out under argon using standard vacuum-line techniques. Solvents were purified by general procedures and freshly distilled prior to use. All other commercially available chemicals were used without further purification. $(NEt_4)_2[M^{II}(SPh)_4]$ (M = Zn, Cd, and Hg) were synthesized according to a modified literature procedure.[38] Ligand precursors, $\{3,6\text{-}(RCONH)_2C_6H_2\text{-}1,2\text{-}S_2\}_2$ (R = $CH_3$, *t*-Bu), were prepared using the previously reported methods.[36]

**$(NEt_4)_2[Zn\{1,2\text{-}S_2\text{-}3,6\text{-}(t\text{-}BuCONH)_2C_6H_2\}_2]$ (1).** $\{3,6\text{-}(t\text{-}BuCONH)_2C_6H_2\text{-}1,2\text{-}S_2\}_2$ (0.500 g, 0.74 mmol) was suspended in 50 mL of methanol, and tetraethylammonium borohydride (0.200 g, 1.4 mmol) was added to give an yellow solution. To this solution, zinc dibromide (0.150 g, 0.67 mmol) in 10 mL of methanol was added dropwise with stirring. The volume of solution was reduced to ca. 5 mL under vacuum, and 50 mL of diethyl ether was added to give an off-white powder. After filtration, this powder was washed with ethyl acetate, water, and diethyl ether and dried under reduced pressure. The solid was recrystallized from acetonitrile/diethyl ether to afford colorless crystals, which were collected by filtration, washed with diethyl ether, and dried to give the product as 0.650 g (97%) of a white powder. IR (KBr): $\nu_{NH}$ 3319, $\nu_{CO}$ 1678 $cm^{-1}$. MS (ESI): *m/z* 741 ($MH^-$). $^1H$ NMR (DMSO-$d_6$, anion) $\delta$: 9.20 (s, 4H), 7.73 (s, 4H), 1.25 (s, 36H). Anal. Calcd for $C_{48}H_{84}N_6O_4S_4Zn\cdot H_2O$: C, 56.47; H, 8.49; N, 8.23. Found: C, 56.46; H, 8.41; N, 8.30.

**$(NEt_4)_2[Cd\{1,2\text{-}S_2\text{-}3,6\text{-}(t\text{-}BuCONH)_2C_6H_2\}_2]$ (2).** This complex was prepared by the same method of **1** using $CdCl_2\cdot 2.5H_2O$. Yield: 96%. IR (KBr): $\nu_{CO}$ 1677 $cm^{-1}$. MS (ESI): *m/z* 791 ($MH^-$). $^1H$ NMR (DMSO-$d_6$, anion) $\delta$: 9.50 (s, 4H), 7.78 (s, 4H), 1.25 (s, 36H). $^{113}Cd$ NMR (DMSO-$d_6$, anion) $\delta$: 809. Anal. Calcd for $C_{48}H_{84}N_6O_4S_4Cd\cdot H_2O$: C, 53.99; H, 8.12; N, 7.87. Found: C, 53.70; H, 8.03; N, 7.84.

**$(NEt_4)_2[Hg^{II}\{1,2\text{-}S_2\text{-}3,6\text{-}(t\text{-}BuCONH)_2C_6H_2\}_2]$ (3).** This complex was prepared by a modified method of **1** using $Hg^{II}Cl_2$. Before the addition of mercury dichloride, acetic acid was added dropwise, cooling in dry ice/methanol bath until evolution of hydrogen gas ceased. Yield: 90%. IR (KBr): $\nu_{NH}$ 3303, $\nu_{CO}$ 1677 $cm^{-1}$. MS (ESI): *m/z* 879 ($MH^-$). $^1H$ NMR (DMSO-$d_6$, anion) $\delta$: 9.36 (s, 4H), 7.77 (s, 4H), 1.25 (s, 36H). $^{199}Hg$ NMR (DMSO-$d_6$, anion) $\delta$: −56. Anal.


(21) Vasak, M.; Kagi, J. H. R.; Hill, H. A. O. *Biochemistry* **1981**, *20*, 2852–2856.
(22) Johnson, B. A.; Armitage, I. M. *Inorg. Chem.* **1987**, *26*, 3139–3144.
(23) Lu, W. H.; Stillman, M. J. *J. Am. Chem. Soc.* **1993**, *115*, 3291–3299.
(24) Jiang, D. T.; Heald, S. M.; Sham, T. K.; Stillman, M. *J. Am. Chem. Soc.* **1994**, *116*, 11004–11013.
(25) Leiva-Presa, A.; Capdevila, M.; Gonzalez-Duarte, P. *Eur. J. Biochem.* **2004**, *271*, 4872–4880.
(26) Chung, W. P.; Dewan, J. C.; Walters, M. A. *J. Am. Chem. Soc.* **1991**, *113*, 525–530.
(27) Chung, W. P.; Dewan, J. C.; Walters, M. A. *Inorg. Chem.* **1991**, *30*, 4280–4282.
(28) Pande, J.; Vasak, M.; Kagi, J. H. R. *Biochemistry* **1985**, *24*, 6717–6722.
(29) Okamura, T.; Ueyama, N.; Nakamura, A.; Ainscough, E. W.; Brodie, A. M.; Waters, J. M. *J. Chem. Soc., Chem. Commun.* **1993**, 1658–1660.
(30) Ueyama, N.; Taniuchi, K.; Okamura, T.; Nakamura, A.; Maeda, H.; Emura, S. *Inorg. Chem.* **1996**, *35*, 1945–1951.
(31) Okamura, T.; Takamizawa, S.; Ueyama, N.; Nakamura, A. *Inorg. Chem.* **1998**, *37*, 18–28.
(32) Ueyama, N.; Inohara, M.; Onoda, A.; Ueno, T.; Okamura, T.; Nakamura, A. *Inorg. Chem.* **1999**, *38*, 4028–4031.
(33) Swenson, D.; Baenziger, N. C.; Coucouvanis, D. *J. Am. Chem. Soc.* **1978**, *100*, 1932–1934.
(34) Garner, C. D.; Nicholson, J. R.; Clegg, W. *Inorg. Chem.* **1984**, *23*, 2148–2150.
(35) Kato, M.; Kojima, K.; Kamura, T. A.; Yamamoto, H.; Yamamura, T.; Ueyama, N. *Inorg. Chem.* **2005**, *44*, 4037–4044.
(36) Baba, K.; Okamura, T.; Suzuki, C.; Yamamoto, H.; Yamamoto, T.; Ohama, M.; Ueyama, N. *Inorg. Chem.* **2006**, *45*, 894–901.
(37) Baba, K.; Okamura, T.; Yamamoto, H.; Yamamoto, T.; Ohama, M.; Ueyama, N. *Inorg. Chem.* **2006**, *45*, 8365–8371.
(38) Ueyama, N.; Sugawara, T.; Sasaki, K.; Nakamura, A.; Yamashita, S.; Wakatsuki, Y.; Yamazaki, H.; Yasuoka, N. *Inorg. Chem.* **1988**, *27*, 741–747.

Calcd for $C_{48}H_{84}N_6O_4S_4Hg \cdot H_2O$: C, 49.87; H, 7.50; N, 7.27. Found: C, 49.75; H, 7.33; N, 7.36. Complex **3** was also prepared using $(NEt_4)[Hg^{II}(SPh)_3]$ instead of $(NEt_4)_2[Hg^{II}(SPh)_4]$ in a high yield (80%).

**$(PPh_4)_2[Zn\{1,2\text{-}S_2\text{-}3,6\text{-}(t\text{-}BuCONH)_2C_6H_2\}_2]$ (4).** A solution of tetraphenylphosphonium bromide (0.334 g, 0.80 mmol) in 10 mL of acetonitrile was added to a solution of **1** (0.200 g, 0.20 mmol) in 10 mL of acetonitrile. This mixture was cooled overnight at 0 °C to give pale yellow crystals. The crystals were collected by filtration, washed with acetonitrile, methanol, and diethyl ether, and dried under reduced pressure to afford the product as 0.270 g of yellow crystals (95%). IR (KBr): $\nu_{NH}$ 3304, $\nu_{CO}$ 1678 $cm^{-1}$. MS (ESI): *m*/*z* 741 ($MH^-$). $^1H$ NMR (DMSO-$d_6$, anion) $\delta$: 9.21 (s, 4H), 7.73 (s, 4H), 1.24 (s, 36H). ($CDCl_3$, anion) $\delta$: 9.31 (s, 4H), 7.84 (s, 4H), 1.13 (s, 36H). Anal. Calcd for $C_{80}H_{84}N_4O_4P_2S_4Zn \cdot H_2O$: C, 66.76; H, 6.02; N, 3.89. Found: C, 66.99; H, 6.13; N, 3.86.

**$(PPh_4)_2[Cd\{1,2\text{-}S_2\text{-}3,6\text{-}(t\text{-}BuCONH)_2C_6H_2\}_2]$ (5).** This complex was prepared by the same method of **4**. Yield: 92%. IR (KBr): $\nu_{NH}$ 3288, $\nu_{CO}$ 1677 $cm^{-1}$. MS (ESI): *m*/*z* 791 ($MH^-$). $^1H$ NMR (DMSO-$d_6$, anion) $\delta$: 9.51 (s, 4H), 7.78 (s, 4H), 1.25 (s, 36H). ($CDCl_3$, anion) $\delta$: 9.59 (s, 4H), 7.92 (s, 4H), 1.15 (s, 36H). Anal. Calcd for $C_{80}H_{84}N_4O_4P_2S_4Cd \cdot 0.5H_2O \cdot 0.5CH_3CN$: C, 64.96; H, 5.82; N, 4.21. Found: C, 64.99; H, 5.67; N, 4.10.

**$(PPh_4)_2[Hg^{II}\{1,2\text{-}S_2\text{-}3,6\text{-}(t\text{-}BuCONH)_2C_6H_2\}_2]$ (6).** This complex was prepared by a similar method of **4** using **3**. Yield: 94%. IR (KBr): $\nu_{CO}$ 1677 $cm^{-1}$. MS (ESI): *m*/*z* 879 ($MH^-$). $^1H$ NMR (DMSO-$d_6$, anion) $\delta$: 9.36 (s, 4H, NH), 7.76 (s, 4H, arom), 1.25 (s, 36H, *t*-Bu). ($CDCl_3$, anion) $\delta$: 9.42 (s, 4H), 7.91 (s, 4H), 1.13 (s, 36H). Anal. Calcd for $C_{80}H_{84}N_4O_4P_2S_4Hg \cdot H_2O$: C, 61.03; H, 5.51; N, 3.56. Found: C, 61.24; H, 5.26; N, 3.46.

**$(NEt_4)_2[Zn\{1,2\text{-}S_2\text{-}3,6\text{-}(CH_3CONH)_2C_6H_2\}_2]$ (7).** $\{3,6\text{-}(CH_3CONH)_2C_6H_2\text{-}1,2\text{-}S_2\}_2$ (0.20 g, 0.39 mmol) was suspended in 50 mL of methanol, and 10 mL of dimethylformamide and $NEt_4BH_4$ (0.25 g, 1.72 mmol) was added to give a clear yellow solution. To this solution, zinc dibromide (0.080 g, 0.36 mmol) in 10 mL of methanol was added dropwise with stirring. The volume of the solution was reduced to ca. 10 mL under vacuum, and 50 mL of diethyl ether was added to give a cream−yellow powder. After filtration, this powder was washed with ethyl acetate and diethyl ether and dried in vacuo. The product was recrystallized from methanol to afford 0.26 g of product (88%) as beige needles. IR (KBr): $\nu_{NH}$ 3290, $\nu_{CO}$ 1677 $cm^{-1}$. MS (ESI): *m*/*z* 573 ($MH^-$). $^1H$ NMR (DMSO-$d_6$, anion) $\delta$: 8.84 (s, 4H), 7.57 (s, 4H), 2.06 (s, 12H). Anal. Calcd for $C_{36}H_{60}N_6O_4S_4Hg \cdot 1.5H_2O$: C, 50.19; H, 7.37; N, 9.75. Found: C, 50.18; H, 7.32; N, 9.84.

**$(NEt_4)_2[Cd\{1,2\text{-}S_2\text{-}3,6\text{-}(CH_3CONH)_2C_6H_2\}_2]$ (8).** This complex was prepared by the same method of **7** using $CdCl_2 \cdot 2.5H_2O$. Yield: 90%. IR (KBr): $\nu_{NH}$ 3276, $\nu_{CO}$ 1685 $cm^{-1}$. MS (ESI): *m*/*z* 622 ($MH^-$). $^1H$ NMR (DMSO-$d_6$, anion) $\delta$: 9.12 (s, 4H), 7.62 (s, 4H), 2.07 (s, 12H). Anal. Calcd for $C_{36}H_{60}N_6O_4S_4Cd \cdot 2H_2O$: C, 47.12; H, 7.03; N, 9.16. Found: C, 47.05; H, 7.22; N, 9.25.

**$(NEt_4)_2[Hg^{II}\{1,2\text{-}S_2\text{-}3,6\text{-}(CH_3CONH)_2C_6H_2\}_2]$ (9).** This complex was prepared by a modified method of **7** using $Hg^{II}Cl_2$. Yield: 85%. IR (KBr): $\nu_{NH}$ 3276, $\nu_{CO}$ 1685 $cm^{-1}$. MS (ESI): *m*/*z* 711 ($MH^-$). $^1H$ NMR (DMSO-$d_6$, anion) $\delta$: 9.03 (s, 4H), 7.57 (s, 4H), 2.06 (s, 12H). Anal. Calcd for $C_{36}H_{60}N_6O_4S_4Hg \cdot H_2O$: C, 43.77; H, 6.33; N, 8.51. Found: C, 43.64; H, 6.02; N, 8.42.

**$(NEt_4)[Hg^{II}\{1,2\text{-}S_2\text{-}3,6\text{-}(t\text{-}BuCONH)_2C_6H_2\}\{S\text{-}2\text{-}(t\text{-}BuCONH)_2C_6H_2SC(t\text{-}Bu)N\}]$ (10).** This complex was prepared by a modified method of **3**. Before the addition of mercury dichloride, acetic acid was added dropwise in excess. Yield: 90%. MS (ESI): *m*/*z* 861 ($M^-$). $^1H$ NMR (DMSO-$d_6$, anion) $\delta$: 9.20 (s, 1H), 8.79 (s, 2H), 8.30 (d, 1H), 7.69 (d, 2H), 7.68 (s, 2H), 1.46 (s, 9H), 1.32 (s, 9H), 1.23 (s, 18H). Anal. Calcd for $C_{48}H_{84}N_6O_4S_4Hg$: C, 48.49; H, 6.41; N, 7.07. Found: C, 48.14; H, 6.34; N, 7.05.

**$(NEt_4)_2[Zn(1,2\text{-}S_2C_6H_4)_2]$ (11).** $(NEt_4)_2[Zn(SC_6H_5)_4]$ (0.29 g, 0.38 mmol) was dissolved in 10 mL of methanol. To this solution, 1,2-benzenedithiol (90 $\mu$L, 0.78 mmol) was added. The volume of the solution was reduced to ca. 5 mL under vacuum, and then 50 mL of diethyl ether was added to give an off-white powder. After filtration, this powder was washed with diethyl ether and dried in vacuo. The product was recrystallized from acetonitrile/diethyl ether to afford 0.18 g of product (78%) as colorless needles. MS (ESI): *m*/*z* 345 ($MH^-$). $^1H$ NMR (DMSO-$d_6$, anion) $\delta$: 7.17 (dd, 2H), 6.37 (dd, 2H). Anal. Calcd for $C_{28}H_{48}N_2S_4Zn \cdot H_2O$: C, 53.86; H, 8.07; N, 4.49. Found: C, 53.90; H, 7.97; N, 4.56.

**$(NEt_4)_2[Cd(1,2\text{-}S_2C_6H_4)_2]$ (12).** This complex was prepared as colorless needles by the same method of **11** using $(NEt_4)_2[Cd(SC_6H_5)_4]$. Yield: 72%. MS (ESI): *m*/*z* 395 ($MH^-$). $^1H$ NMR (DMSO-$d_6$, anion) $\delta$: 7.29 (dd, 2H), 6.38 (dd, 2H). $^{113}Cd$ NMR (DMSO-$d_6$, anion) $\delta$: 821. Anal. Calcd for $C_{28}H_{48}N_2S_4Cd \cdot H_2O$: C, 50.09; H, 7.51; N, 4.17. Found: C, 50.28; H, 7.48; N, 4.40.

**$(NEt_4)_2[Hg^{II}(1,2\text{-}S_2C_6H_4)_2]$ (13).** This complex was prepared as colorless needles by the same method of **11** using $(NEt_4)_2[Hg^{II}(SC_6H_5)_4]$. Yield: 66%. MS (ESI): *m*/*z* 483 ($MH^-$). $^1H$ NMR (DMSO-$d_6$, anion) $\delta$: 7.34 (dd, 2H), 6.37 (dd, 2H). $^{199}Hg$ NMR (DMSO-$d_6$, anion) $\delta$: −11. Anal. Calcd for $C_{28}H_{48}N_2S_4Hg \cdot 4Et_2O \cdot 3CH_3CN \cdot 4H_2O$: C, 48.70; H, 8.58; N, 5.68. Found: C, 48.60; H, 8.89; N, 5.73.

**$(NEt_4)_2[Hg^{II}_2(1,2\text{-}S_2C_6H_4)_3]$ (14).** This complex was prepared as colorless needles by a 1:2 reaction of $(NEt_4)[Hg^{II}(SC_6H_5)_3]$ and 1,2-benzenedithiol. Yield: 64%. MS (ESI): *m*/*z* 823 ($MH^-$). $^1H$ NMR (DMSO-$d_6$, anion) $\delta$: 7.54 (dd, 2H), 6.69 (dd, 2H). $^{199}Hg$ NMR (DMSO-$d_6$, anion) $\delta$: −128. Anal. Calcd for $C_{34}H_{52}N_2S_6Hg_2$: C, 37.73; H, 4.84; N, 2.59. Found: C, 37.78; H, 4.72; N, 2.71.

**$[Hg^{II}_6\{1,2\text{-}S_2\text{-}3,6\text{-}(t\text{-}BuCONH)_2C_6H_2\}_6]$ (15).** $Hg^{II}(SPh)_2$ (250 mg, 0.60 mmol) and $\{3,6\text{-}(t\text{-}BuCONH)_2C_6H_2\text{-}1,2\text{-}S_2\}_2$ (200 mg, 0.30 mmol) were suspended in 50 mL of THF. During reflux for 1 h, the suspension gradually turned to a clear yellow solution. It was allowed to stand at ambient temperature to give yellow crystals. After filtration, the crystals were washed with THF and dried under reduced pressure. Yield: 120 mg (37%). IR (KBr): $\nu_{NH}$ 3326, $\nu_{CO}$ 1677, 1640 $cm^{-1}$. MS (ESI): *m*/*z* 711 ($MH^-$). $^1H$ NMR (DMSO-$d_6$) $\delta$: 8.7–9.0 (12H), 7.5–7.8 (12H), 1.1–1.3 (108H). $^1H$ NMR ($CDCl_3$) $\delta$: 8.71 (s, 6H), 8.27 (d, 6H), 7.61 (s, 6H), 7.43 (d, 6H), 1.21 (s, 54H), 1.34 (s, 54H). Anal. Calcd. for $C_{96}H_{132}N_{12}O_{12}S_{12}Hg_6 \cdot$ THF: C, 36.32; H, 4.27; N, 5.08. Found: C, 36.15; H, 4.06; N, 5.08.

**Physical Measurements.** $^1H$, $^{113}Cd$, and $^{199}Hg$ NMR spectra were obtained with a Jeol ALPHA-600 in chloroform-*d* or DMSO-$d_6$ at 27 °C. $^1H$ NMR chemical shifts are referenced to $SiMe_4$ as an internal standard. $^{113}Cd$ and $^{199}Hg$ NMR chemical shifts were referenced to 50 mM of $Cd(ClO_4)_2$ in $D_2O$ and $Hg^{II}Cl_2$ in DMSO-$d_6$ [−1500 ppm[39] relative to $Hg(CH_3)_2$] as an external standard, respectively. IR spectra were taken using a Jasco FT/IR-8300 spectrometer. Samples were prepared as KBr pellets. Mass spectrometric analyses were performed on FinniganMAT LCQ and LCQ DECA electrospray mass spectrometers.

**X-ray Structure and Determination.** Data collection was performed on a Rigaku RAXIS-RAPID Imaging Plate diffractometer using graphite monochromated Mo K$\alpha$ radiation (0.71069

(39) Bharara, M. S.; Parkin, S.; Atwood, D. A. *Inorg. Chem.* **2006**, *45*, 7261–7268.

**Table 1.** Crystallographical Data for **4**·$CH_3OH$, **5**·0.5$CH_3CN$, **6**·0.5$CH_3CN$, **13**·0.75$CH_3CN$·$H_2O$, **14**, and **15**·3THF

| | **4**·$CH_3OH$ | **5**·0.5$CH_3CN$ | **6**·0.5$CH_3CN$ | **13**·0.75$CH_3CN$·$H_2O$ | **14** | **15**·3THF |
|---|---|---|---|---|---|---|
| formula | $ZnS_4P_2O_5N_4C_{81}H_{88}$ | $CdS_4P_2O_4N_{4.5}C_{81}H_{85.5}$ | $HgS_4P_2N_{4.5}O_4C_{81}H_{85.5}$ | $HgS_4N_{2.75}OC_{29.50}H_{52.25}$ | $Hg_2S_6N_2C_{34}H_{52}$ | $Hg_6S_{12}N_{12}O_{15}C_{108}H_{156}$ |
| fw | 1453.18 | 1488.69 | 1576.87 | 790.34 | 1082.34 | 3450.75 |
| cryst syst | monoclinic | monoclinic | monoclinic | triclinic | monoclinic | trigonal |
| space group | $P2_1/c$ | $P2_1/c$ | $P2_1/c$ | $P\bar{1}$ | $P2_1/c$ | $R\bar{3}c$ |
| $a$ (Å) | 20.0998(6) | 17.1271(7) | 17.1067(6) | 17.0547(7) | 9.0312(3) | 19.3024(3) |
| $b$ (Å) | 16.9986(5) | 19.6683(7) | 19.6670(8) | 17.6005(6) | 33.116(1) | 19.3024(3) |
| $c$ (Å) | 29.5969(5) | 22.430(1) | 22.387(1) | 14.0856(6) | 14.6456(5) | 19.3024(3) |
| α (deg) | 90 | 90 | 90 | 98.064(2) | 90 | 76.5928(3) |
| $\beta$ (deg) | 131.872(1) | 94.114(1) | 94.132(1) | 112.208(2) | 114.727(2) | 76.5928(3) |
| $\gamma$ (deg) | 90 | 90 | 90 | 97.144(1) | 90 | 76.5928(3) |
| $V$ (Å) | 7530.0(3) | 7536.2(5) | 7512.1(5) | 3802.5(3) | 3978.5(2) | 6683.5(2) |
| $Z$ | 4 | 4 | 4 | 4 | 4 | 2 |
| $d_{calcd}$ (g $cm^{-1}$) | 1.282 | 1.233 | 1.394 | 1.380 | 1.807 | 1.715 |
| $\mu$ ($mm^{-1}$) | 0.533 | 0.496 | 2.260 | 4.301 | 8.069 | 7.130 |
| GOF ($F^2$) | 1.00 | 0.909 | 1.03 | 1.05 | 1.00 | 1.07 |
| $R1^a$ [$I > 2\sigma(I)$] | 0.077 | 0.055 | 0.045 | 0.057 | 0.034 | 0.045 |
| $wR2^b$ (all data) | 0.203 | 0.049 | 0.112 | 0.163 | 0.073 | 0.086 |

$^a$ $R1 = \sum||F_o| - |F_c||/\sum|F_o|$. $^b$ $wR2 = \{\sum[w(F_o^2 - F_c^2)^2]/\sum[w(F_o^2)^2]\}^{1/2}$.

Å). The structures were solved using SHELXS-86[40] (**6**·0.5$CH_3CN$), SHELXS-97[40] (**5**·0.5$CH_3CN$, **13**·0.75$CH_3CN$·$H_2O$, **14**, and **15**·3THF), or SIR92[41] (**4**·$CH_3OH$) and refined by the use of the teXsan[42] crystallographic software package. Nonhydrogen atoms were refined anisotropically. All hydrogen atoms were located at the calculated positions and included in the least-squares calculations. The final refinement was carried out using full-matrix least-squares using SHELXL-97.[43] The final difference Fourier map showed no significant features. Atom scattering factors and dispersion corrections were taken from the International Table.[44] These basic crystallographic parameters are listed in Table 1.

**Computational Methods.** The DFT calculations at the PBE1PBE[45] level were carried out using the Gaussian03 program package.[46] Computations in the present study were carried out on a SGI Altix 3700 at the Computer Center for Agriculture, Forestry, and Fisheries Research, MAFF, Japan. The atomic coordinates from X-ray structures of **4**−**6** were used as the initial structure. The *t*-Bu groups were replaced by $CH_3$ groups to reduce the time for calculation. After the full geometry optimizations using aug-cc-pVTZ-PP[47,48] for Zn, Cd, and Hg, aug-cc-pVTZ[49] for S, and cc-pVDZ[50,51] basis sets for all other atoms, vibrational frequency calculations were carried out to ensure that the stationary points located on the potential energy surfaces by geometry optimization were minima. For benzendithiolate complexes, $[M^{II}(1,2\text{-}S_2C_6H_4)_2]^{2-}$ (M = Zn, Cd, Hg), DFT calculations were also performed. The initial structures were derived from X-ray structures of **4**−**6**. DFT calculations were also performed using B3LYP functional and various basis sets (see the Supporting Information). The bonding properties of the NH···S hydrogen bond were analyzed using the natural bond orbital (NBO) program,[52] and the NBO View was used for orbital visualizations. Atomic charges were derived from natural population analysis (NPA).[53]

The computer software package, MOE,[54] was used for analysis of hydrogen bonding in proteins.

## Results and Discussion

**Synthesis.** The procedures for the syntheses of $(A)_2[M^{II}\{1,2\text{-}S_2\text{-}3,6\text{-}(RCONH)_2C_6H_2\}_2]$ [A = $NEt_4$, R = *t*-Bu, M = Zn (**1**); A = $NEt_4$, R = *t*-Bu, M = Cd (**2**); A = $NEt_4$, R = *t*-Bu, M = Hg (**3**); A = $PPh_4$, R = *t*-Bu, M = Zn (**4**); A = $PPh_4$, R = *t*-Bu, M = Cd (**5**); A = $PPh_4$, R = *t*-Bu, M = Hg (**6**); A = $NEt_4$, R = $CH_3$, M = Zn (**7**); A = $NEt_4$, R = $CH_3$, M = Cd (**8**); A = $NEt_4$, R = $CH_3$, M = Hg (**9**)] are shown in parts a and b of Scheme 1. The ligand precursor, $\{3,6\text{-}(RCONH)_2C_6H_2\text{-}1,2\text{-}S_2\}_2$ (R = $CH_3$ and *t*-Bu), was reduced by $BH_4^-$ in methanol or methanol/DMF solution, and then $ZnBr_2$ or $CdCl_2$·2.5$H_2O$ was added to the solution. For Hg complexes, acetic acid was added before the addition of $Hg^{II}Cl_2$ to prevent the reduction of $Hg^{II}$ (Scheme 1b). The dithiol 3,6-$(RCONH)_2C_6H_2$-1,2-$(SH)_2$ that was generated by


(40) Sheldrick, G. M. *SHELXS-86 and SHELXS-97: Structure Solving Programs*; University of Göttingen: Göttingen, Germany, 1986 and 1997.

(41) Altomare, A.; Cascaano, G.; Giacovazzo, C.; Guagliardi, A.; Burla, M. C.; Polidori, G.; Camalli, M. *J. Appl. Crystallogr.* **1994**, *27*, 435–450.

(42) *teXsan: Crystal Structure Analysis Program*; Molecular Structure Corporation, **1985** and **2004**.

(43) Sheldrick, G. M. *SHELXL-97*; University of Göttingen: Göttingen, Germany, 1997.

(44) Cromer, D. T.; Waber, J. T. *International Tables for X-ray Crystallography*; Kynoch Press: Birmingham, U.K. 1974; Vol. *4*.

(45) Perdew, J. P.; Burke, K.; Ernzerhof, M. *Phys. Rev. Lett.* **1997**, *78*, 1396–1396.

(46) Frisch, M. J. ; Trucks, G. W.; Schlegel, H. B.; Scuseria, G. E.; Robb, M. A.; Cheeseman, J. R.; Montgomery, J. A., Jr., Vreven, T.; Kudin, K. N.; Burant, J. C.; Millam, J. M.; Iyengar, S. S.; Tomasi, J.; Barone, V.; Mennucci, B.; Cossi, M.; Scalmani, G.; Rega, N.; Petersson, G. A.; Nakatsuji, H.; Hada, M.; Ehara, M.; Toyota, K.; Fukuda, R.; Hasegawa, J.; Ishida, M.; Nakajima, T.; Honda, Y.; Kitao, O.; Nakai, H.; Klene, M.; Li, X.; Knox, J. E.; Hratchian, H. P.; Cross, J. B.; Bakken, V.; Adamo, C.; Jaramillo, J.; Gomperts, R.; Stratmann, R. E.; Yazyev, O.; Austin, A. J.; Cammi, R.; Pomelli, C.; Ochterski, J. W.; Ayala, P. Y.; Morokuma, K.; Voth, G. A.; Salvador, P.; Dannenberg, J. J.; Zakrzewski, V. G.; Dapprich, S.; Daniels, A. D.; Strain, M. C.; Farkas, O.; Malick, D. K.; Rabuck, A. D.; Raghavachari, K.; Foresman, J. B.; Ortiz, J. V.; Cui, Q.; Baboul, A. G.; Clifford, S.; Cioslowski, J.; Stefanov, B. B.; Liu, G.; Liashenko, A.; Piskorz, P.; Komaromi, I.; Martin, R. L.; Fox, D. J.; Keith, T.; Al-Laham, M. A.; Peng, C. Y.; Nanayakkara, A.; Challacombe, M.; Gill, P. M. W.; Johnson, B.; Chen, W.; Wong, M. W.; Gonzalez, C.; Pople, J. A. *Gaussian 03, Revision B.04*; Gaussian, Inc.: Wallingford, CT, 2004.

(47) Peterson, K. A.; Puzzarini, C. *Theor. Chem. Acc.* **2005**, *114*, 283–296.

(48) Schuchardt, K. L.; Didier, B. T.; Elsethagen, T.; Sun, L.; Gurumoorthi, V.; Chase, J.; Li, J.; Windus, T. L. *J. Chem. Inf. Model.* **2007**, *47*, 1045–1052.

(49) Dunning, T. H. *J. Chem. Phys.* **1989**, *90*, 1007–1023.

(50) Woon, D. E.; Dunning, T. H. *J. Chem. Phys.* **1993**, *98*, 1358–1371.

(51) Kendall, R. A.; Dunning, T. H.; Harrison, R. J. *J. Chem. Phys.* **1992**, *96*, 6796–6806.

(52) Glendening, E. D.; Reed, A. E.; Carpenter, J. E.; Weinhold, F. *NBO, version 3.1*.

(53) Reed, A. E.; Weinhold, F. *J. Chem. Phys.* **1983**, *78*, 4066–4073.

(54) *Molecular Operating Environment (MOE)*; Chemical Computing Group, Inc.: Montreal, Canada, 2005.

**Scheme 1.** Synthetic Routes for Zn, Cd, and Hg Complexes

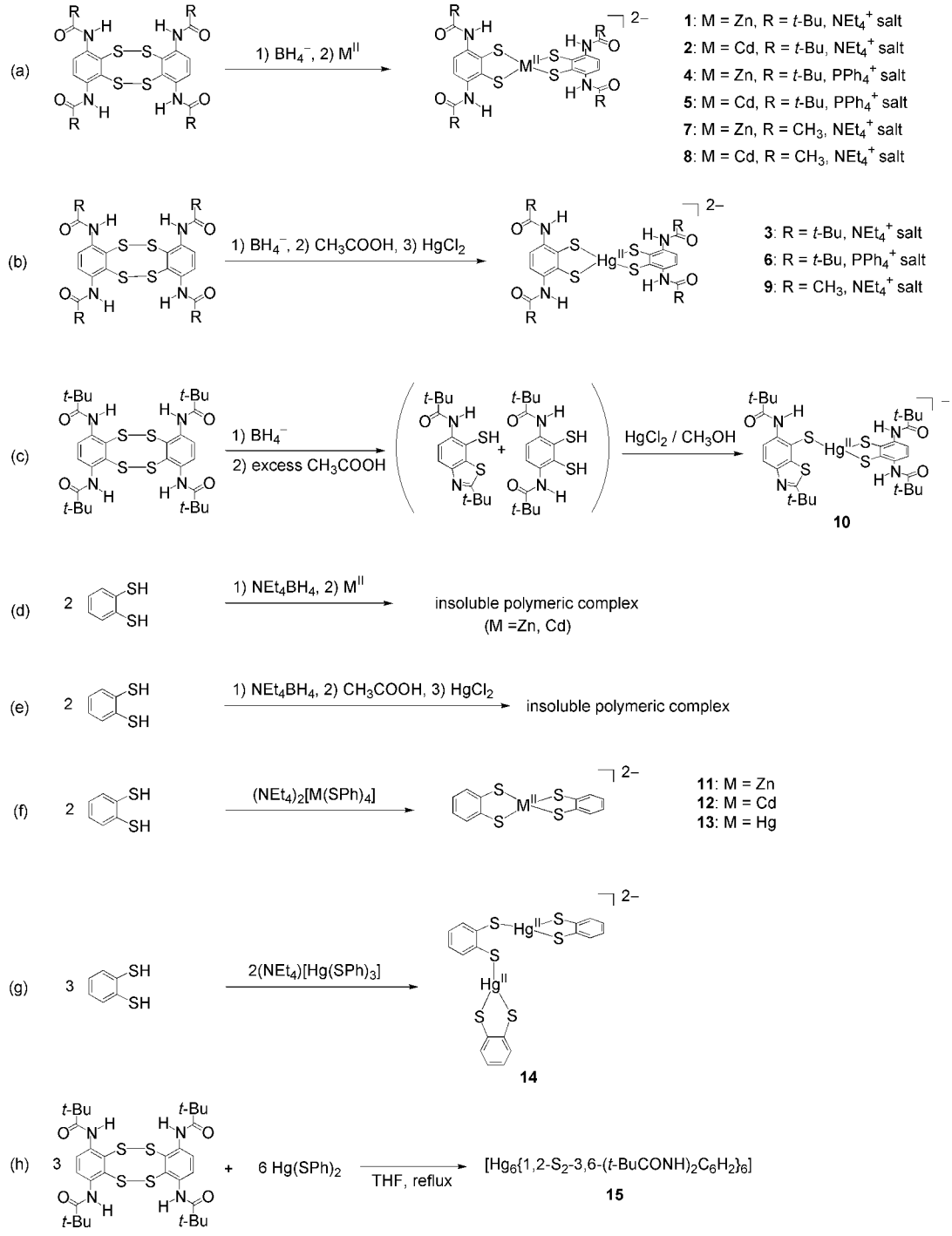


the reduction of $\{3,6\text{-}(RCONH)_2C_6H_2\text{-}1,2\text{-}S_2\}_2$ followed by acidification is unstable in solution because of the intramolecular condensation that results in the formation of benzothiazole derivatives, such as 1-SH-2-$RCONHC_6H_2SC$(*t*-Bu)N and $C_6H_2\{SC(t\text{-}Bu)N\}_2$. When acetic acid was added in excess, $(NEt_4)[Hg^{II}\{1,2\text{-}S_2\text{-}3,6\text{-}(t\text{-}BuCONH)_2C_6H_2\}\{S\text{-}2\text{-}t\text{-}BuCONHC_6H_2SC(t\text{-}Bu)N\}]$ (**10**) (Scheme 1c) was isolated.

$(NEt_4)_2[M^{II}(1,2\text{-}S_2C_6H_4)_2]$ (M = Zn, Cd, and Hg) could not be isolated using $1,2\text{-}C_6H_4(SH)_2$ by the same procedure as that used for $[M^{II}\{1,2\text{-}S_2\text{-}3,6\text{-}(RCONH)_2C_6H_2\}_2]^{2-}$ because of the formation of unknown insoluble precipitates in organic solvents, such as DMF, DMSO, $CH_3CN$, and $CH_3OH$. Presumably, these precipitates are polymeric complexes of the type $[\{M^{II}(1,2\text{-}S_2C_6H_4)\}_n]$ (parts d and e of Scheme 1). Bustos et al. could not synthesize $(NEt_4)_2[Cd(tdt)_2]$ (tdt = toluene-3,4-dithiolate) but isolated $(AsPh_4)_2[Cd(tdt)_2]$, which is considered to exhibit special stability in the $AsPh_4^+/[Cd(tdt)_2]^{2-}$ lattice.[55] We used a new procedure for the synthesis of $(NEt_4)_2[M^{II}(1,2\text{-}S_2C_6H_4)_2]$ [M = Zn (**11**), Cd (**12**) and Hg (**13**)] in which the mononuclear complexes

(55) Bustos, L.; Khan, M. A.; Tuck, D. G. *Can. J. Chem.* **1983**, *61*, 1146–1152.

$(NEt_4)_2[M^{II}(SPh)_4]$ (M = Zn, Cd, Hg) were used as the starting materials (Scheme 1f). In this route, $(NEt_4)_2[M^{II}(1,2\text{-}S_2C_6H_4)_2]$ was isolated as crystals in a high yield.

Other mercury compounds such as $(NEt_4)[Hg^{II}(SPh)_3]$ and $Hg^{II}(SPh)_2$ were also used as staring materials. When $(NEt_4)[Hg^{II}(SPh)_3]$ was used as the starting material, a dinuclear complex $(NEt_4)_2[Hg^{II}_2(1,2\text{-}S_2C_6H_4)_3]$ (**14**) was isolated as crystals in a high yield (Scheme 1g); however, not $(NEt_4)_2[Hg^{II}_2(1,2\text{-}S_2\text{-}3,6\text{-}(t\text{-}BuCONH)_2C_6H_2)_3]$ but **3** was isolated. A hexanuclear mercury complex $[Hg^{II}_6\{1,2\text{-}S_2\text{-}3,6\text{-}(t\text{-}BuCONH)_2C_6H_2\}_6]$ (**15**) was synthesized by refluxing a suspension of $Hg^{II}(SPh)_2$ and $\{3,6\text{-}(t\text{-}BuCONH)_2C_6H_2\text{-}1,2\text{-}S_2\}_2$ in THF (Scheme 1h). Both $Hg^{II}(SPh)_2$ and the ligand precursor were hardly soluble in THF. However, during the reflux, the suspension gradually turned to a clear yellow solution. On the other hand, a light-yellow solid immediately precipitated from a stirred solution of 1,2-benzenedithiol in THF by the dropwise addition of a suspension of $Hg^{II}(SPh)_2$ in THF. The precipitate, which has a metal/ligand ratio of 1 (on the basis of the elemental analysis), is insoluble in organic solvents, such as THF, $CH_3CN$, $CHCl_3$, and $CH_3OH$, even upon heating. The poor solubility suggested the formation of polymeric structures. When using $\{3,6\text{-}(t\text{-}BuCONH)_2C_6H_2\text{-}1,2\text{-}S_2\}_2$, polymerization is prevented by the bulky *t*-BuCONH groups.

**Crystal Structures.** Complexes **4**·$CH_3OH$, **5**·$0.5CH_3CN$, **6**·$0.5CH_3CN$, and **13**·$0.75CH_3CN$·$H_2O$ were structurally characterized. Single crystals of **11** and **12** could not be removed from the solvent because the crystal solvents were easily lost during the treatment. Figure 1 shows the anionic units. The structural parameters are listed in Table 2. All of the complexes possess distorted tetrahedral geometries. The intramolecular N···S distances in **4**·$CH_3OH$, **5**·$0.5CH_3CN$, and **6**·$0.5CH_3CN$ are approximately 2.89 Å and the dihedral angles of C15−C16−N1−C17, C14−C13−N2−C27, C35−C36−N3−C37, and C34−C33−N4−C47 are in the range of +24° to −26°, which suggests the presence of NH···S hydrogen bonds. The amide NH does not show any other inter- or intramolecular hydrogen bond.

The mean Zn−S bond length of **4**·$CH_3OH$ is similar to that of $(PPh_4)_2[Zn(mnt)_2]$ (**16**)[56] (mnt = maleonitriledithiolate). The mean Cd−S bond length of **5**·$0.5CH_3CN$ is similar to that (2.508 Å) of $(AsPh_4)_2[Cd(tdt)_2]$·$C_2H_5OH$ (**17**·$C_2H_5OH$),[55] which is a structurally characterized monomeric $Cd^{II}$ dithiolate complex. The mean Hg−S bond length of **6**·$0.5CH_3CN$ is similar to that of **13**·$0.75CH_3CN$·$H_2O$. No significant contribution of the NH···S hydrogen bond to the Hg−S bond lengths, as reported for $(NEt_4)_2[Hg^{II}(S\text{-}2\text{-}CH_3NHCOC_6H_4)_4]$,[35] is observed. The M−S and S−C bond distances and S−M−S angles of **5**·$0.5CH_3CN$ and **6**·$0.5CH_3CN$ are very similar. In comparison to the structures of **4**·$CH_3OH$, **5**·$0.5CH_3CN$, and **6**·$0.5CH_3CN$, it is seen that the lengths of the Cd−S and Hg−S bonds are significantly longer than that of the Zn−S bond, which is consistent with the difference in the covalent bond radii (Zn, 131; Cd, 148;

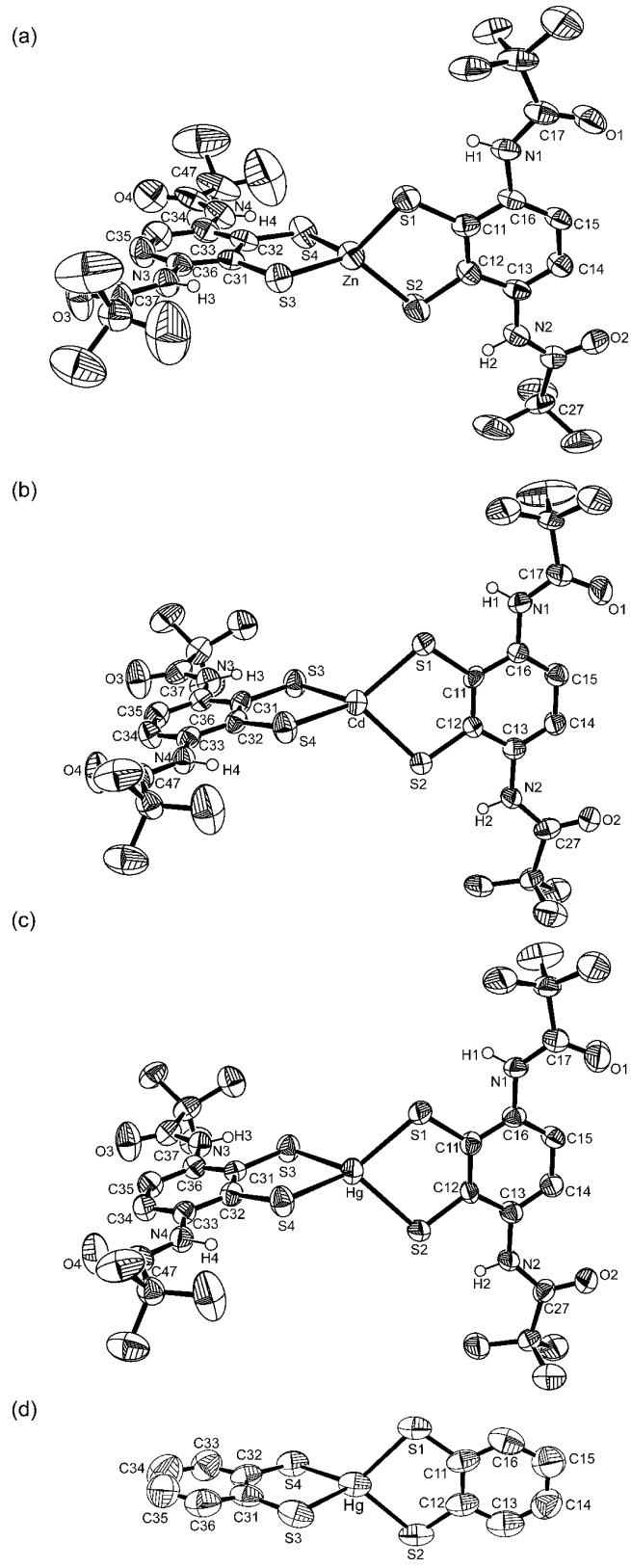


**Figure 1.** ORTEP drawings of (a) $(PPh_4)_2[Zn\{1,2\text{-}S_2\text{-}3,6\text{-}(t\text{-}BuCONH)_2C_6H_2\}_2]$·$CH_3OH$ (**4**·MeOH), (b) $(PPh_4)_2[Cd\{1,2\text{-}S_2\text{-}3,6\text{-}(t\text{-}BuCONH)_2C_6H_2\}_2]$·$0.5(CH_3CN)$ (**5**·$0.5CH_3CN$), (c) $(PPh_4)_2[Hg^{II}\{1,2\text{-}S_2\text{-}3,6\text{-}(t\text{-}BuCONH)_2C_6H_2\}_2]$ (**6**·$0.5CH_3CN$), and (d) $(NEt_4)_2[Hg^{II}(1,2\text{-}S_2C_6H_4)_2]$·$0.75CH_3CN$·$H_2O$ (**13**·$0.75CH_3CN$·$H_2O$) (anion unit). Thermal motion is represented by 50% probability ellipsoids. The amide protons are placed on the calculated positions.

(56) Lewis, G. R.; Dance, I. *J. Chem. Soc., Dalton Trans.* **2000**, 3176–3185.

**Table 2.** Selected Intra- and Intermolecular Distances (Å) and Bond Angles (deg) of **4**·$CH_3OH$, **5**·0.5$CH_3CN$, **6**·0.5$CH_3C$, **13**·0.75$CH_3CN$···$H_2O$[a], $(PPh_4)_2[Zn(mnt)_2]$ (**16**) (mnt = maleonitriledithiolate),[56] and $(AsPh_4)_2[Cd(tdt)_2]$·$C_2H_5OH$ (**17**·$C_2H_5OH$)[55]

| | **4**·$CH_3OH$ | **16** | **5**·0.5$CH_3CN$ | **17**·$C_2H_5OH$ | **6**·0.5$CH_3CN$ | **13**·0.75$CH_3CN$·$H_2O$ |
|---|---|---|---|---|---|---|
| M−S1 | 2.318(3) | 2.341 | 2.500(1) | 2.510 | 2.496(1) | 2.508(2) |
| M−S2 | 2.316(2) | 2.316 | 2.502(1) | 2.490 | 2.523(1) | 2.531(3) |
| M−S3 | 2.324(2) | 2.333 | 2.510(1) | 2.502 | 2.520(1) | 2.500(2) |
| M−S4 | 2.324(2) | 2.341 | 2.507(1) | 2.531 | 2.506(1) | 2.524(3) |
| mean | 2.320 | 2.333 | 2.505 | 2.508 | 2.511 | 2.516 |
| S1−C11 | 1.768(8) | 1.743 | 1.762(4) | 1.761 | 1.768(4) | 1.75(1) |
| S2−C12 | 1.76(1) | 1.739 | 1.768(4) | 1.790 | 1.766(4) | 1.741(9) |
| S3−C31 | 1.780(7) | 1.725 | 1.776(4) | 1.756 | 1.764(4) | 1.74(1) |
| S4−C32 | 1.73(1) | 1.742 | 1.771(4) | 1.772 | 1.762(4) | 1.767(9) |
| mean | 1.76 | 1.737 | 1.769 | 1.770 | 1.765 | 1.750 |
| S1−M−S2 | 91.6(1) | 94.08 | 85.51(3) | 87.27 | 85.32(4) | 87.00(8) |
| S3−M−S4 | 91.62(10) | 93.24 | 85.84(3) | 86.16 | 85.53(4) | 87.18(9) |
| mean | 91.61 | 93.66 | 85.68 | 86.72 | 85.43 | 87.09 |
| C15−C16−N1−C17 | −1.0(9) | | −25.4(6) | | −25.7(7) | |
| C14−C13−N2−C27 | −8.8(8) | | 22.9(6) | | 24.2(7) | |
| C35−C36−N3−C37 | 8.0(9) | | 3.7(6) | | 5.0(7) | |
| C34−C33−N4−C47 | 7(1) | | −9.1(6) | | −9.0(7) | |
| metal−dithiolate fold angle[b] in M−S1−S2−C11−C12 | 8.63 | 5.98 | 15.31 | 11.60 | 16.06 | 8.49 |
| metal−dithiolate fold angle in M−S3−S4−C31−C32 | 3.39 | 14.71 | 6.94 | 16.35 | 7.34 | 7.03 |
| mean N···S | 2.895 | | 2.885 | | 2.881 | |

[a] One of two molecules in the asymmetric unit was compared. [b] It was defined as the angle between S−M−S and S−C−C−S dithiolate planes.

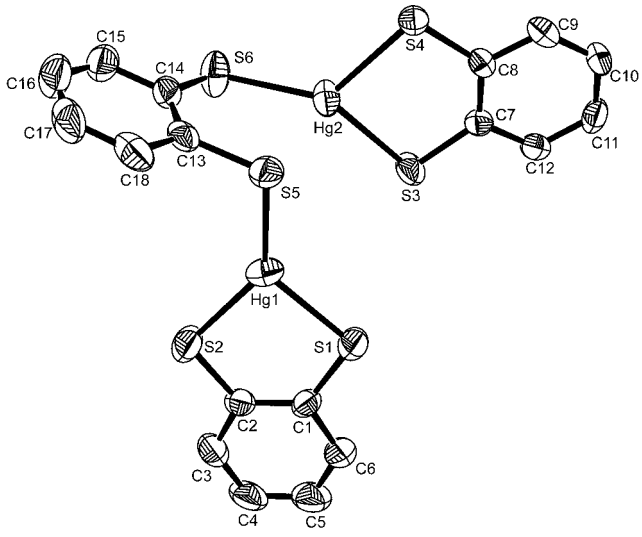


**Figure 2.** ORTEP drawing of $(NEt_4)_2[Hg^{II}_2(1,2\text{-}S_2C_6H_4)_2]$ (**14**) (anionic unit). Thermal motion is represented by 50% probability ellipsoids. The amide protons are placed on the calculated positions.

and Hg, 148 pm).[57] The metal−dithiolate fold angles[58] between the S−C−C−S and S−M−S planes are similar to those in **16**, **17**·$C_2H_5OH$, and **13**·0.75$CH_3CN$·$H_2O$. No distinct tendencies of the fold angle could be found among these crystal structures. However, as seen in **5**·0.5$CH_3CN$ and **6**·0.5$CH_3CN$, a large fold angle induced a large C−C−N−C dihedral angle.

Figure 2 shows the molecular structure of the anionic unit of **14**. The structural parameters of **14** are listed in Table 3. This unique dimeric structure is slightly similar to that of a previously reported complex $[Hg^{II}_2$(5,6-diphenyl-1,4-dithiacyclohexadiene-2,3-dithiolate)$_3]^{2-}$.[59] The two Hg centers are in different coordination environments. The geometry of Hg1 in **14** is distorted trigonal planar, as observed in three-coordinated $Hg^{II}$ thiolate complexes.[60] The distance between Hg1 and S1−S2−S5 plane is 0.075 Å. The three Hg−S bonds are almost within the usual range (2.4–2.5 Å) of the three-coordinated $Hg^{II}$ thiolate complexes.[61,62] The S1−Hg1−S2 and S3−Hg2−S4 bite angles are are larger than those of **13**·0.75$CH_3CN$·$H_2O$ because of the relatively short Hg−S bond lengths in **14**. The interligand S1−Hg1−S5 and S2−Hg1−S5 bond angles are larger than those of **13**·0.75$CH_3CN$·$H_2O$. The geometry around Hg2 is distorted trigonal pyramidal with a long Hg2···S5 bond coordinated at the apical position. The distance between the Hg2 and S3S4S6 plane is 0.303 Å. The Hg2−S3, Hg2−S4, and Hg2−S6 bond lengths are within the usual range of three-coordinated $Hg^{II}$ thiolate complexes. The interligand S3−Hg2−S6 and S4−Hg2−S6 angles are similar to those of Hg1.

The structural parameters of **15**·3THF are listed in Table 4. The cluster framework consists of 6 Hg atoms and 12 S atoms from the six dithiolate ligands (Figure 3a). The cluster has a crystallographic $\bar{3}$ symmetry axis at the center and $^1/_6$ of **15**·3THF, $Hg^{II}\{1,2\text{-}S_2\text{-}3,6\text{-}(t\text{-}BuCONH)_2C_6H_2\}$·0.5THF, is in the asymmetric unit. The reported hexanuclear $Hg^{II}$ thiolate complexes have additional oxygen or halogen atoms as coordinating atoms.[63–65] Akdas reported a hexanuclear $Hg^{II}$ complex with only sulfur (thiolate and thioether) atoms

(57) Pauling, L. *The Nature of the Chemical Bond*; Cornell University Press: New York, 1939.
(58) Joshi, H. K.; Cooney, J. J. A.; Inscore, F. E.; Gruhn, N. E.; Lichtenberger, D. L.; Enemark, J. H. *Proc. Natl. Acad. Sci. U.S.A.* **2003**, *100*, 3719–3724.
(59) Noh, D. Y.; Underhill, A. E.; Hursthouse, M. B. *Chem. Commun.* **1997**, 2211–2212.
(60) Wright, J. G.; Natan, M. J.; Macdonnell, F. M.; Ralston, D. M.; O'Halloran, T. V. *Prog. Inorg. Chem.* **1990**, *38*, 323–412.
(61) Santos, R. A.; Gruff, E. S.; Koch, S. A.; Harbison, G. S. *J. Am. Chem. Soc.* **1991**, *113*, 469–475.
(62) Gruff, E. S.; Koch, S. A. *J. Am. Chem. Soc.* **1990**, *112*, 1245–1247.
(63) Alsina, T.; Clegg, W.; Fraser, K. A.; Sola, J. *J. Chem. Soc., Chem. Commun.* **1992**, 1010–1011.
(64) Casas, J. S.; Montero-Vazquez, P.; Sanchez, A.; Sordo, J.; Vazquez-Lopez, E. M. *Polyhedron* **1998**, *17*, 2417–2424.
(65) Bharara, M. S.; Bui, T. H.; Parkin, S.; Atwood, D. A. *Inorg. Chem.* **2005**, *44*, 5753–5760.

**Table 3.** Selected Intra- and Intermolecular Distances (Å) and Bond Angles (deg) of **14**

| | | | |
|---|---|---|---|
| Hg1−S1 | 2.437(1) | S1−Hg1−S2 (bite angle) | 90.26(5) |
| Hg1−S2 | 2.429(2) | S3−Hg2−S4 (bite angle) | 88.92(4) |
| Hg1−S5 | 2.382(1) | | |
| Hg2−S3 | 2.461(1) | S1−Hg1−S5 | 130.26(5) |
| Hg2−S4 | 2.487(1) | S2−Hg1−S5 | 139.16(5) |
| Hg2−S6 | 2.425(1) | S3−Hg2−S6 | 138.45(6) |
| Hg2···S5 | 2.824(2) | S4−Hg2−S6 | 127.54(5) |
| S1−C1 | 1.771(6) | S1···S2 | 3.448 |
| S2−C2 | 1.761(5) | S3···S4 | 3.465 |
| S3−C7 | 1.757(5) | S5···S6 | 3.441 |
| S4−C8 | 1.763(5) | | |
| S5−C13 | 1.787(5) | | |
| S6−C14 | 1.747(7) | | |

**Table 4.** Selected Intra- and Intermolecular Distances (Å) and Bond Angles (deg) of **15**·3THF[a]

| | | | |
|---|---|---|---|
| Hg−S2 | 2.378(1) | C5−C6−N1−C11 | −35.1(9) |
| Hg−S1′ | 2.401(2) | C4−C3−N2−C21 | −90.4(7) |
| Hg···S1 | 2.817(2) | | |
| Hg···S2′ | 3.122(2) | S1−Hg−S2 | 82.87(5) |
| Hg···O2″ | 2.686(5) | S1−Hg−S1′ | 98.811(9) |
| Hg···Hg′ | 3.838 | S1−Hg−S2″ | 157.25 |
| S1−C1 | 1.774(6) | S1−Hg−O2″ | 123.74 |
| S2−C2 | 1.774(6) | S2−Hg−S1′ | 178.12(5) |
| | | S2−Hg−S2″ | 85.51 |
| S1···S2 | 3.453 | S2−Hg−O2″ | 95.74 |
| N1···S1 | 2.906 | S1′−Hg−S2″ | 92.62 |
| N2···S2 | 2.924 | S1′−Hg−O2″ | 84.05 |
| N2···O1‴ (intermolecular) | 2.955 | S2″−Hg−O2″ | 76.81 |

[a] ′, $-y+1, -z, -x+1$; ″, $z+1, x-1, y$; ‴, $-x+{}^3/_2, -z+{}^1/_2, -y+1$.

as coordinating atoms.[66] The cluster framework resembles a hexanuclear $Pd^{II}$ complex with dithiolate ligands.[67] $Hg^{II}$ covalently binds to S2 and S1′ with a linear geometry (Figure 3b). These bonds are significantly longer than those (2.320–2.348 Å) of the other two-coordinate $Hg^{II}$ thiolate complexes $Hg^{II}$(S-2-$SiMe_3C_6H_4$)$_2$ and $Hg^{II}$(S-2,4,6-*i*-$Pr_3C_6H_2$)$_2$.[62,68] The long covalent Hg−S2 and Hg−S1′ bonds are probably caused by the intramolecular contacts between Hg and S1, S2″, and O″ of the neighboring ligands (Figure 3b). The Hg···S1, Hg···S2″, and Hg···O″ distances are between the sum of the covalent radii (Hg−S, 2.52 Å; Hg−O, 2.14 Å)[57] and the sum of the van der Waals radii (Hg···S, 3.35 Å; Hg···O, 3.07 Å).[69] This suggests the presence of bonding Hg···S and Hg···O interactions. The intra- and intermolecular Hg···O interactions of the amide CO groups have also been reported for $Hg^{II}${S-2,6-(*t*-BuCONH)$_2C_6H_3$}$_2$.[30]

The 3D framework (Figure 3c) contains two types of small channels (A and B) along the $C_3$ axis: one (A) passes through the center of the cluster and the other (B) passes through the center of the triangle formed by three neighboring clusters. THF molecules are included in the latter channel. Each cluster is linked to the adjacent clusters by two NH···O=C hydrogen bonds (Figure 3d). The presence of intramolecular N1H1···S1 hydrogen bond is suggested by a short N1···S1 distance and a relatively small C5−C6−N1−C11 dihedral angle. On the other hand, N2H2 does not direct to S2 with a large C4−C3−N2−C21 angle but forms an intermolecular N2−H2···O1‴=C11‴ hydrogen bond, where the N2···O1‴ distance is short (2.955 Å) and the dihedral angle N2−H2···O1‴=C11‴ is 144.9°.

**IR Spectra.** Table 5 lists the IR bands in the amide $\nu$(NH) regions for **1–9** compared to the free $\nu$(NH) regions of the analogous disulfides (S-2-RCONH$C_6H_4$)$_2$ (R = $CH_3$, *t*-Bu) in $CH_2Cl_2$ as standard values[70] because the corresponding ligand precursors {1,2-$S_2$-3,6-(RCONH)$_2C_6H_2$}$_2$ (R = $CH_3$ and *t*-Bu) are insoluble in less polar organic solvents, such as $CH_3CN$ and $CH_2Cl_2$, and possess intermolecular NH···O=C hydrogen bonds in the solid state. The large differences ($\Delta\nu$(NH) = −78 to −111 $cm^{-1}$) in the NH bands between the complexes (**1–9**) and the corresponding disulfides strongly suggest the formation of the NH···S hydrogen bond, which agrees with the crystallographic structures of **4**·$CH_3OH$, **5**·0.5$CH_3CN$, and **6**·0.5$CH_3CN$.

The $\nu$(NH) of four-coordinated **6** was observed at a much lower wavenumber than that of the two-coordinated complex having NH···S hydrogen bonds, $Hg^{II}$(S-2-*t*-BuCONH$C_6H_4$)$_2$·0.5$H_2O$ [$\nu$(NH) = 3345 $cm^{-1}$].[30] Four-coordinated complexes have stronger NH···S hydrogen bonds than the two-coordinated complexes because of the greater negative charge on the sulfur atom. This large shift of $\nu$(NH) is similar to the shifts $\Delta\nu$(NH) (−108 $cm^{-1}$) in (N$Et_4$)$_2$[$Co^{II}$(S-2-*t*-BuCONH$C_6H_4$)$_4$][34] and $\Delta\nu$(NH) (−94 $cm^{-1}$) in (N$Et_4$)$_2$[$Hg^{II}$(S-2-$CH_3$NHCO$C_6H_4$)$_4$].[35]

The $\Delta\nu$(NH) of Zn complex **1** possessing pivaloylamino groups is less than that of **7** having acetylamino groups by 14 $cm^{-1}$. Similarly, the $\Delta\nu$(NH) values of Cd and Hg complexes **2** and **3** are less than those of **8** and **9** by 10 and 12 $cm^{-1}$, respectively. These results suggest the presence of weaker NH···S hydrogen bonds induced by the electron-donating *t*-butyl groups.

Complexes **4–6** with $PPh_4^+$ countercations have a lower $\nu$(NH) as compared to **1–3** that have $NEt_4^+$ ions. The crystal structures revealed that the Ph groups of $PPh_4^+$ are located at a position where Ph can interact with the S and carbonyl O atoms. In contrast to complexes **1–3**, which are colorless, complexes **4–6** are yellow, suggesting some interaction between $PPh_4^+$ and [$M^{II}$\{1,2-$S_2$-3,6-(*t*-BuCONH)$_2C_6H_2$\}$_2$]$^{2-}$.

Interestingly, the $\Delta\nu$(NH) values of the Cd (**2** and **8**) and Hg (**3** and **9**) complexes are less than those of the corresponding Zn complexes **1** and **7** by 14–16 $cm^{-1}$. These results suggest that the NH···S hydrogen bonds in the Cd and Hg complexes are stronger than those in the Zn complexes.

Cluster **15** exhibits a broad $\nu$(NH) band and two $\nu$(C=O) bands at 1677 and 1640 $cm^{-1}$. The higher $\nu$(C=O) band corresponds to the reported free $\nu$(C=O) (1679 $cm^{-1}$) of the pivaloylamino group.[69] The $\nu$(NH) band of **15** is shifted to a lower wavenumber by 63 $cm^{-1}$ from that of a free $\nu$(NH). On the basis of the crystallographic analysis of **15**·3THF, the $\nu$(NH) bands forming NH···S and NH···O=C hydrogen bonds probably overlap, resulting in a broadband close to

(66) Akdas, H.; Graf, E.; Hosseini, M. W.; De Cian, A.; Bilyk, A.; Skelton, B. W.; Koutsantonis, G. A.; Murray, I.; Harrowfield, J. M.; White, A. H. *Chem. Commun.* **2002**, 1042–1043.
(67) Beswick, C. L.; Terroba, R.; Greaney, M. A.; Stiefel, E. I. *J. Am. Chem. Soc.* **2002**, *124*, 9664–9665.
(68) Block, E.; Brito, M.; Gernon, M.; McGowty, D.; Kang, H. K.; Zubieta, J. *Inorg. Chem.* **1990**, *29*, 3172–3181.
(69) Bondi, A. *J. Phys. Chem.* **1964**, *86*, 441–451.
(70) Ueyama, N.; Nishikawa, N.; Yamada, Y.; Okamura, T.; Oka, S.; Sakurai, H.; Nakamura, A. *Inorg. Chem.* **1998**, *37*, 2415–2421.

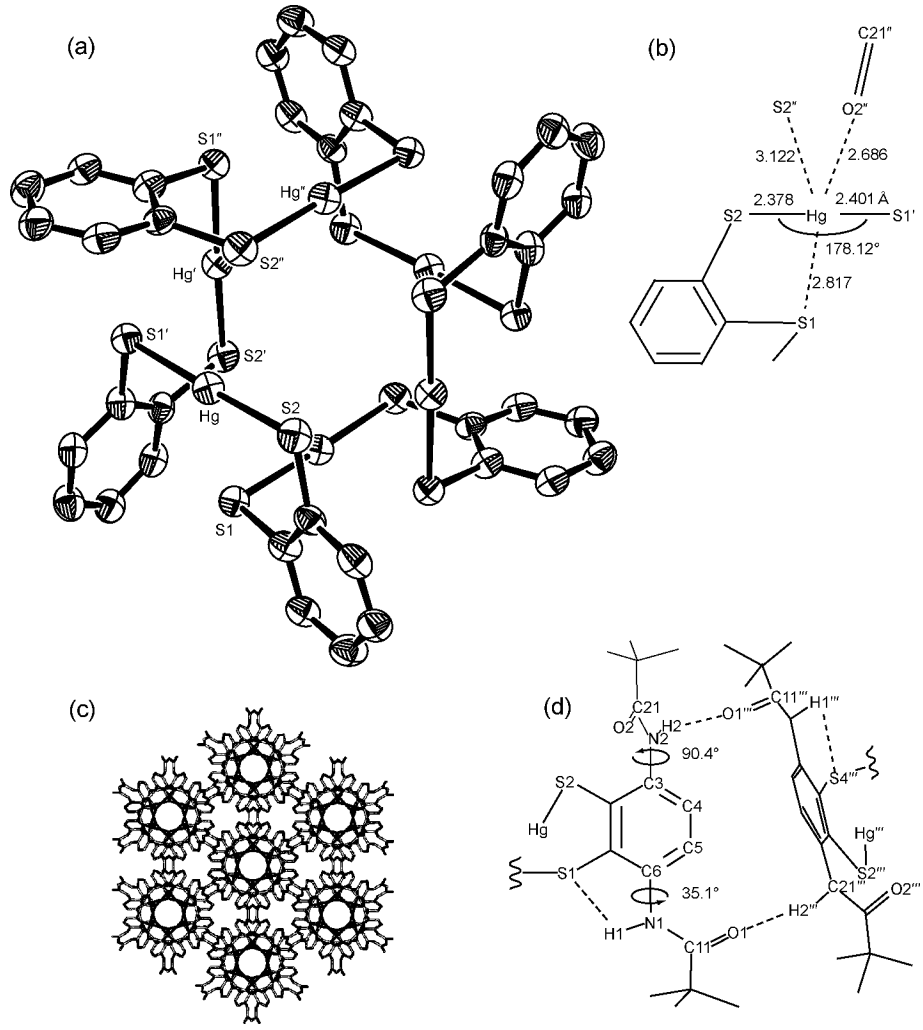


**Figure 3.** (a) ORTEP drawing of $[Hg^{II}_6\{1,2\text{-}S_2\text{-}3,6\text{-}(t\text{-}BuCONH)_2C_6H_2\}_6]\cdot 3THF$ (**15**·3THF). The pivaloylamino groups, THF molecules, and H atoms are omitted for clarity. Thermal motion is represented by 50% probability ellipsoids. The amide protons are placed on the calculated positions. (b) Coordination geometry around the mercury center (Å and deg). (c) Crystal packing structure of **15**·3THF. The methyl groups of pivaloyl substituents, THF molecules, and H atoms are omitted for clarity. (d) Intermolecular NH···O═C and intramolecular NH···S hydrogen bonds.

**Table 5.** IR Bands of $\nu$(NH) in **1**–**9** in the Solid State, the Shifts from Those of the Corresponding Disulfides, $(S\text{-}2\text{-}RCONHC_6H_4)_2$[a], in $CH_2Cl_2$ solution, and the Chemical Shifts of Amide Proton in DMSO-$d_6$ ($CDCl_3$)

| | metal | ligand | cation | $\nu$(NH) ($cm^{-1}$) | $\Delta\nu$(NH) ($cm^{-1}$) | $\delta$(NH) (ppm) |
|---|---|---|---|---|---|---|
| **1** | Zn | *t*-Bu | $NEt_4$ | 3319 | −78 | 9.20 |
| **2** | Cd | *t*-Bu | $NEt_4$ | 3301 | −96 | 9.50 |
| **3** | Hg | *t*-Bu | $NEt_4$ | 3303 | −94 | 9.36 |
| **4** | Zn | *t*-Bu | $PPh_4$ | 3304 | −93 | 9.20 (9.31) |
| **5** | Cd | *t*-Bu | $PPh_4$ | 3288 | −109 | 9.50 (9.59) |
| **6** | Hg | *t*-Bu | $PPh_4$ | 3286 | −111 | 9.36 (9.42) |
| **7** | Zn | $CH_3$ | $NEt_4$ | 3290 | −92 | 8.84 (8.70) |
| **8** | Cd | $CH_3$ | $NEt_4$ | 3276 | −106 | 9.12 (8.97) |
| **9** | Hg | $CH_3$ | $NEt_4$ | 3276 | −106 | 9.03 (8.72) |
| **15** | Hg | *t*-Bu | | 3326 | −71 | 8.7−9.0 |

[a] $\nu$(NH) values for R = $CH_3$ and *t*-Bu are 3382 and 3397 $cm^{-1}$, respectively, in 10 mM $CH_2Cl_2$.

3345 $cm^{-1}$ of $Hg^{II}\{S\text{-}2\text{-}(t\text{-}BuCONH)C_6H_4\}_2\cdot 0.5H_2O$ with an intramolecular NH···S hydrogen bond.[30] The lower $\nu$(C═O) band at 1640 $cm^{-1}$ is ascribed to the intermolecular NH···O═C hydrogen bond, which was anticipated from the crystal structure.

**$^1$H NMR Spectra.** The $^1$H NMR chemical shifts of the amide hydrogens, i.e., $\delta$(NH) of **1**–**9** are listed in Table 5. Complexes **1**–**9** showed sharp signals for amide hydrogens because of suppressed ligand dissociation equilibrium, which is different from a broad NH signal of $(NEt_4)_2[Hg^{II}(S\text{-}2\text{-}CH_3NHCOC_6H_4)_4]$,[35] The $\delta$(NH) of $(NEt_4)_2[Hg^{II}(S\text{-}2\text{-}CH_3\text{-}NHCOC_6H_4)_4]$ was 9.20 ppm in $CDCl_3$, which is near those of **6** and **9**. Their values were between a thiolate, $(NEt_4)(S\text{-}2\text{-}t\text{-}BuNHCOC_6H_4)$ (12.16 ppm), and a disulfide, $(2\text{-}t\text{-}BuNHCOC_6H_4S)_2$ (5.83 ppm), in $CDCl_3$ and reasonable to NH···S hydrogen-bonding amide proton in metal complexes. The order of $\delta$(NH) values, Cd > Hg > Zn, in all of the complexes with the same ligands suggests the order of the strength of intramolecular NH···S hydrogen bonds in solution, which disagrees with the order Hg ≈ Cd > Zn expected from the IR data in the solid. The $\delta$(NH) of **3** and **8** in DMSO-$d_6$ shifted upfield by 0.14 and 0.09 ppm from the corresponding Cd complexes, **2** and **9**, respectively. In $CDCl_3$ solution, the same trend was observed. The additional coordination of a solvent molecule to Cd may reduce the donation from the thiolates, resulting in stronger NH···S hydrogen bonds. Sandström et al. have reported that the Cd

(71) Stalhandske, C. M. V.; Persson, I.; Sandström, M.; Kamienska-Piotrowicz, E. *Inorg. Chem.* **1997**, *36*, 3174–3182.

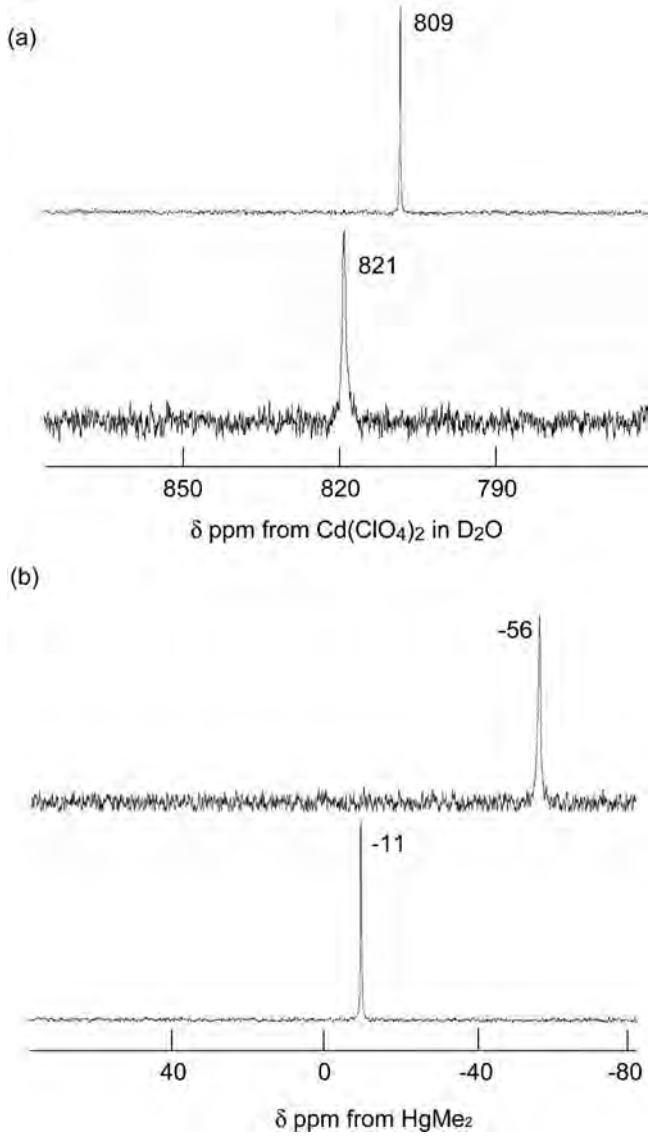


**Figure 4.** (a) $^{113}$Cd NMR of $(NEt_4)_2[Cd\{1,2\text{-}S_2\text{-}3,6\text{-}(t\text{-}BuCONH)_2C_6H_2\}_2]$ (**2**) (upper) and $(NEt_4)_2[Cd(1,2\text{-}S_2C_6H_4)_2]$ (**12**) (lower) in DMSO-$d_6$. (b) $^{199}$Hg NMR of $(NEt_4)_2[Hg^{II}\{1,2\text{-}S_2\text{-}3,6\text{-}(t\text{-}BuCONH)_2C_6H_2\}_2]$ (**3**) (upper) and $(NEt_4)_2[Hg^{II}(1,2\text{-}S_2C_6H_4)_2]$ (**13**) (lower) in DMSO-$d_6$.

ion is coordinated by six thiolates in *N*,*N*-dimethylthioformamide, although Zn and Hg ions are coordinated by four thiolates.[71]

The dissociation of cluster **15** was observed by $^1$H NMR and mass spectral measurements. The $^1$H NMR spectra in dimethylsulfoxide-$d_6$ showed multiple amide and aromatic proton signals at 8.7−9.0 and 7.5−7.8 ppm, respectively. ESI−MS spectra in a mixture of dimethylformamide and acetonitrile indicated peaks at *m*/*z* 1101.3 (22%), 1640.1 (100%), 2179.5 (64%), 2718.0 (20%), 3257.8 (68%), and 3796.9 (18%) in the range *m*/*z* 250−4000. Each peak corresponds to $\{Hg^{II}1,2\text{-}S_2\text{-}3,6\text{-}(t\text{-}BuCONH)_2C_6H_2\}_n + Na^+$ ($n$ = 2−7). These results suggest the occurrence of some equilibrium processes in the solution.

**$^{113}$Cd and $^{199}$Hg NMR Spectra.** Figure 4 shows the $^{113}$Cd and $^{199}$Hg NMR spectra of **2**, **3**, **12**, and **13**. The chemical-shift values are reasonable for four-coordinated thiolates.[60,72,73] The signals are close to –19 ppm of $[Hg^{II}(toluene\text{-}3,4\text{-}dithiolate)_2]^{2-}$.[74] The monodentate complex $(NEt_4)_2[Hg^{II}(S\text{-}2\text{-}CH_3NHCOC_6H_4)_4]$ showed a signal at −466 from $Hg(CH_3)_2$,[35] which suggests the dissociation of the ligand to form two- or three-coordinated complexes.

For example, the two-coordinated complex $Hg^{II}(S\text{-}2\text{-}t\text{-}BuCONHC_6H_4)_2$ shows a $^{199}$Hg signal at a higher field [−1142 ppm from $Hg(CH_3)_2$].[30] The downfield shift of the $^{199}$Hg NMR signal is caused by an increase in the electron donation from S(p$\pi$) to an unoccupied Hg(p), which should increase with the coordination number.[35,75,76] The contribution of the intramolecular hydrogen bond to the $^{199}$Hg chemical shift was described in the previous paper related $Hg^{II}(S\text{-}2\text{-}t\text{-}BuCONHC_6H_4)_2$, where the hydrogen bond decreases the S to Hg charge transfer, resulting in a high-field shift.[30] The signal of **3** was shifted upfield from that of **13** by 45 ppm. In a similar manner, the $^{113}$Cd NMR signal of **2** was shifted upfield from that of **12** by 12 ppm. In metallothionein, the $^{113}$Cd signals are found in the range of 600–700 ppm. The variations in the chemical shifts are probably caused by the NH···S hydrogen bonds in addition to the coordination mode, number, and geometry.

Complex **14** had only one $^{199}$Hg signal at −128 ppm from $Hg(CH_3)_2$, which was expected from only one set of $^1$H NMR signals. The chemical shift was in the range from −354 ppm[72] of $[Hg(SC_6H_5)_3]^-$ to −11 ppm of **13**, which may suggest that each Hg atom of **14** is equally coordinated by three sulfur atoms and in a dissociation-rebinding equilibrium for the Hg−S bond as shown in Figure S1 in the Supporting Information.

**DFT Calculations.** The nature of the NH···S hydrogen bonds in a series of metal complexes was investigated using DFT calculations. Calculations with a hybrid PBE1PBE function showed better agreement with the experimental data than with the tested combinations of the B3LYP function and other basis sets (Table S1 in the Supporting Information). The optimized M−S and S−C bond lengths, S−M−S, metal−dithiolate fold angles, amide−benzene dihedral angles, and the calculated NH stretching vibrations are shown in Table 6. The M−S and S−C lengths are in good agreement with the experimental values. The optimized M−S lengths of $[M^{II}(1,2\text{-}S_2\text{-}3,6\text{-}(CH_3CONH)_2C_6H_2)]_2]^{2-}$ are shorter by 0.013–0.020 Å than those of $[M^{II}(1,2\text{-}S_2C_6H_4)_2]^{2-}$, which was not clearly seen in the crystal structure analysis of **6**·0.5 $CH_3CN$ and **13**·0.75$CH_3CN$·$H_2O$. DFT calculations indicate that the Hg complex with large fold angles also has large mean amide−benzene dihedral angles, as found in crystal structures. The calculated NH stretchings frequencies in Cd and Hg complexes are shifted to lower wavenumbers by 13–19 cm$^{-1}$ from the frequency of the Zn complex, which is in good agreement with the experimental IR data. The character of the intramolecular hydrogen bond was analyzed using NBO analysis, as reported in small organic com-

(72) Natan, M. J.; Millikan, C. F.; Wright, J. G.; O'Halloran, T. V. *J. Am. Chem. Soc.* **1990**, *112*, 3255–3257.
(73) Goodfellow, B. J.; Lima, M. J.; Ascenso, C.; Kennedy, M.; Sikkink, R.; Rusnak, F.; Moura, I.; Moura, J. J. G. *Inorg. Chim. Acta* **1998**, *273*, 279–287.

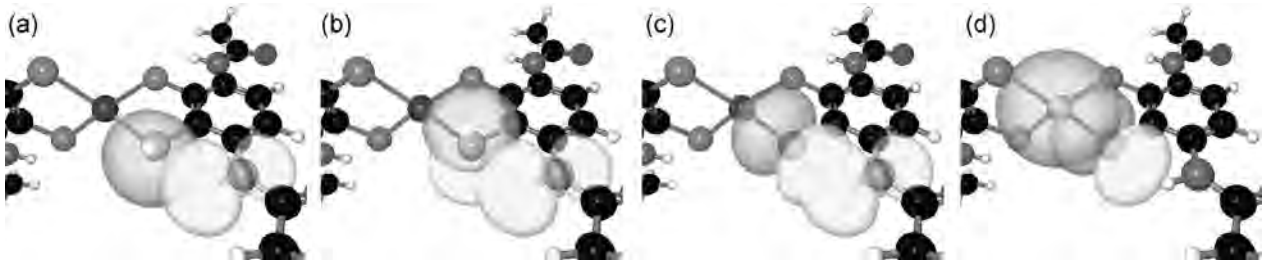


**Figure 5.** Preorthogonal NBOs (PNBOs) of NH···S hydrogen bonds at the PBE1PBE/SDD fully optimized geometry of $(NEt_4)_2[Cd\{1,2\text{-}S_2\text{-}3,6\text{-}(CH_3CONH)_2C_6H_2\}_2]$: (a) $n_S(1) \rightarrow \sigma_{NH}^*$, (b) $n_S(2) \rightarrow \sigma_{NH}^*$, (c) $n_S(3) \rightarrow \sigma_{NH}^*$, and (d) $n_S(3) \rightarrow s_{Cd}^*$. For clarity, only PNBOs of an amide group and a sulfur atom are shown.

**Table 6.** Full Optimized Data of $[M^{II}(daabdt)_2]^{2-}$ (daabdt = $1,2\text{-}S_2\text{-}3,6\text{-}(CH_3CONH)_2C_6H_2$) and $[M^{II}(bdt)]^{2-}$ (bdt = $1,2\text{-}S_2C_6H_4$) (M = Zn, Cd, Hg)

| | Zn | | Cd | | Hg | |
|---|---|---|---|---|---|---|
| ligand | daabdt | bdt | daabdt | bdt | daabdt | bdt |
| mean M−S (Å) | 2.333 | 2.351 | 2.519 | 2.539 | 2.544 | 2.557 |
| mean S−C (Å) | 1.761 | 1.752 | 1.765 | 1.756 | 1.763 | 1.754 |
| mean fold angle (deg) | 0.11 | 0 | 1.90 | 0 | 18.54 | 0 |
| mean amide−benzene angle (deg)[a] | 0.33 | | 0.36 | | 3.14 | |
| NH stretching ($cm^{-1}$) | 3438 | | 3424 | | 3419 | |

[a] It was defined as the absolute value of the dihedral angle $\theta$, C−C−N−C(=O) ($0 \le \theta < 180°$).

**Table 7.** CT Energies from Sulfur Lone Pairs ($n_S$) to Antibonding N−H Orbitals ($\sigma_{NH}^*$) and NPA Charge on S in $[M^{II}\{1,2\text{-}S_2\text{-}3,6\text{-}(CH_3CONH)_2C_6H_2\}_2]^{2-}$ (M = Zn, Cd, Hg)

| | Zn | Cd | Hg |
|---|---|---|---|
| | Total CT Energy (kcal $mol^{-1}$) | | |
| $n_S(1) \rightarrow \sigma_{NH}^*$ | 30.2 | 30.9 | 27.4 |
| $n_S(2) \rightarrow \sigma_{NH}^*$ | 0 | 0.4 | 10.8 |
| $n_S(3) \rightarrow \sigma_{NH}^*$ | 24.8 | 31.2 | 24.3 |
| total $n_S \rightarrow \sigma_{NH}^*$ | 55.0 | 62.5 | 62.5 |
| | Averaged p Character (%) | | |
| $n_S(1)$ | 27.0 | 24.5 | 23.6 |
| $n_S(2)$ | 99.9 | 99.9 | 99.9 |
| $n_S(3)$ | 91.6 | 94.3 | 95.1 |
| NPA charge on S | −0.514 | −0.526 | −0.473 |

pounds.[77–79] The second-order perturbation theory analysis of the off-diagonal matrix in the NBO basis indicates that the three charge transfers (CTs) are the major sources of the NH···S hydrogen bonds (Table 7 and Figure 5). These CTs occur from the s-type [$n_S(1)$] and two p-type sulfur lone pairs [$n_S(2)$ and $n_S(3)$]. The lobes of $n_S(2)$ and $n_S(3)$ are perpendicular and parallel to the benzene ring, respectively. The stronger NH···S hydrogen bonding in the Cd complex as compared to the Zn complex is due to the larger $n_S(3) \rightarrow \sigma_{NH}^*$ energy. The p character of $n_S(3)$ in the Cd complex is larger than that in the Zn complex. As shown in Figure 5, because the lobe of $n_S(3)$ is directed to the metal-unfilled s orbital ($s_M^*$) and $\sigma_{NH}^*$, the enhancement of the p character to bind the Cd atom with a longer bond distance than Zn would increase the spatial overlap between the $n_S(3)$ and $\sigma_{NH}^*$ orbitals. Such increased overlap in the Cd complex was supported by the larger off-diagonal element of $n_S(3) \rightarrow \sigma_{NH}^*$ than that in the Zn complex (Table S2 in the Supporting Information). When the fold angle is large, such as that in the Hg complex, the contribution of $n_S(2) \rightarrow \sigma_{NH}^*$ increases and the contributions of $n_S(1) \rightarrow \sigma_{NH}^*$ and $n_S(3) \rightarrow \sigma_{NH}^*$ decrease. The order of the total CT energy is Hg = Cd > Zn, which is in agreement with the IR data. The mean charges on the sulfur atoms obtained by natural population analysis (NPA) suggest that the population of the negative charge on sulfur is not necessarily crucial to the strength of the NH···S hydrogen bond. NBO analysis can also be used to determine the effects of orbital delocalization by deleting the related orbital(s) or specific interactions between the orbitals followed by recalculation of the approximate SCF energy for the hypothetical system.[80] The calculated deletion energies provide a measure of the destabilization caused by deletion of the interactions between the $n_S$ and the $\sigma_{NH}^*$ orbitals. The deletion is more serious in the Cd (86.7 kcal $mol^{-1}$) and Hg (84.5 kcal $mol^{-1}$) complexes as compared to that in the Zn (78.7 kcal $mol^{-1}$) complex, which indicates that the NH···S hydrogen bond stabilizes the Cd and Hg complexes more effectively.

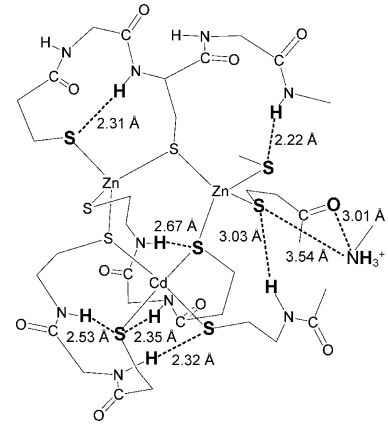


**Figure 6.** Expected NH···S hydrogen bonds in the $\beta$ domain from mammalian metallothionein. The structure was obtained from the X-ray crystal structure (PDB code 4MT2).[19] The positions of amide protons were calculated, and the distances between S and H are shown. The distance between S and N is shown for the ammonium group of lysine.

In metallothionein, the metal-binding sites prefer Zn or Cd ions and it is thought that the size of the metal ions and the metal–thiolate affinities are important factors.[81–84] In the X-ray crystal structure of a $\beta$ domain from a mammalian metallothionein, each metal ion (two Zn and one Cd) is coordinated by two bridging cysteines and two terminal cysteines with a tetrahedral geometry.[19] On the basis of the number and distances of the NH···S hydrogen bonds, the hydrogen-bonded thiolates chose the Cd ion in preference to the Zn ion (Figure 6). Presumably, the Cd complex is more stabilized by the NH···S hydrogen bonds than the Zn complex, as shown by the above computational results. In the case of a high metal/metallothionein ratio containing

bridging sulfur atoms, the decrease in electron donation from ligands to metal ion may also weaken NH···S hydrogen bonds compared to our model complexes. In metallothioneins with a low Hg/metallothionein ratio, the NH···S hydrogen bond is probably one of the factors that stabilizes the four-coordinated Hg by delocalizing the excess negative charge on sulfur atoms and preventing the formation of two- or three-coordinated Hg.

## Conclusion

Mononuclear Zn, Cd, and Hg dithiolate complexes with intramolecular NH···S hydrogen bonds and benzenedithiolate complexes as standard compounds were successfully synthesized. The presence of intramolecular NH···S hydrogen bonds was established by X-ray crystal structures, IR, and NMR spectra. Although significant changes in the M−S bond distances because of the NH···S hydrogen bonds could not be found, NBO analysis suggested the stabilization of the complexes by hydrogen bonding. The experimental and theoretical results revealed that the order of the strength of the hydrogen bonds is Hg, Cd > Zn, which suggests that metallothioneins effectively capture the toxic Cd and Hg ions in biological systems and the capture may also be regulated by the NH···S hydrogen bonds as well as geometry, total charge, and the other factors.

**Acknowledgment.** This work was supported by a Grant-in-Aid from the Ministry of Education, Culture, Sports, Science, and Technology, Japan.

**Supporting Information Available:** X-ray crystallographic files in CIF format, full optimized geometries and NBO analysis using B3LYP functional and various basis sets (Table S1), the detailed second-order perturbation energy analysis (Table S2), a proposed ligand-dissociation equilibrium of **14** (Figure S1), oxidation potentials (Table S3), and cyclic voltammograms (Figure S2 and S3). This material is available free of charge via the Internet at http://pubs.acs.org.

IC702037K

(74) Carson, G. K.; Dean, P. A. W. *Inorg. Chim. Acta* **1982**, *66*, 157–161.
(75) Nakatsuji, H.; Kanda, K.; Endo, K.; Yonezawa, T. *J. Am. Chem. Soc.* **1984**, *106*, 4653–4660.
(76) Hemmingsen, L.; Olsen, L.; Antony, J.; Sauer, S. P. A. *J. Biol. Inorg. Chem.* **2004**, *9*, 591–599.
(77) Alabugin, I. V.; Zeidan, T. A. *J. Am. Chem. Soc.* **2002**, *124*, 3175–3185.
(78) Tian, S. X. *J. Phys. Chem. A* **2006**, *110*, 3961–3966.
(79) Rudner, M. S.; Jeremic, S.; Petterson, K. A.; Kent, D. R.; Brown, K. A.; Drake, M. D.; Goddard, W. A.; Roberts, J. D. *J. Phys. Chem. A* **2005**, *109*, 9076–9082.
(80) Reed, A. E.; Curtiss, L. A.; Weinhold, F. *Chem. Rev.* **1988**, *88*, 899–926.
(81) Nettesheim, D. G.; Engeseth, H. R.; Otvos, J. D. *Biochemistry* **1985**, *24*, 6744–6751.
(82) Good, M.; Hollenstein, R.; Vasak, M. *Eur. J. Biochem.* **1991**, *197*, 655–659.
(83) Pountney, D. L.; Vasak, M. *Eur. J. Biochem.* **1992**, *209*, 335–341.
(84) Chang, C. C.; Huang, P. C. *Protein Eng.* **1996**, *9*, 1165–1172.